



**AFRL-RZ-WP-TP-2008-2032**

**MEASUREMENTS OF NO AND OH CONCENTRATIONS  
IN VITIATED AIR USING DIODE LASER-BASED  
ULTRAVIOLET ABSORPTION SENSORS (POSTPRINT)**

**Thomas N. Anderson, Robert P. Lucht, Terrence R. Meyer, Tarun Mathur,  
Keith D. Grinstead, Jr., James R. Gord, Mark Gruber, and Campbell D. Carter**

**Propulsion Sciences Branch  
Aerospace Propulsion Division**

**DECEMBER 2006**

**Approved for public release; distribution unlimited.**

*See additional restrictions described on inside pages*

**STINFO COPY**

**© 2007 American Institute of Aeronautics and Astronautics, Inc.**

**AIR FORCE RESEARCH LABORATORY  
PROPULSION DIRECTORATE  
WRIGHT-PATTERSON AIR FORCE BASE, OH 45433-7251  
AIR FORCE MATERIEL COMMAND  
UNITED STATES AIR FORCE**

<b>REPORT DOCUMENTATION PAGE</b>				<i>Form Approved</i> OMB No. 0704-0188			
The public reporting burden for this collection of information is estimated to average 1 hour per response, including the time for reviewing instructions, searching existing data sources, gathering and maintaining the data needed, and completing and reviewing the collection of information. Send comments regarding this burden estimate or any other aspect of this collection of information, including suggestions for reducing this burden, to Department of Defense, Washington Headquarters Services, Directorate for Information Operations and Reports (0704-0188), 1215 Jefferson Davis Highway, Suite 1204, Arlington, VA 22202-4302. Respondents should be aware that notwithstanding any other provision of law, no person shall be subject to any penalty for failing to comply with a collection of information if it does not display a currently valid OMB control number. <b>PLEASE DO NOT RETURN YOUR FORM TO THE ABOVE ADDRESS.</b>							
<b>1. REPORT DATE (DD-MM-YY)</b> December 2006		<b>2. REPORT TYPE</b> Conference Paper Postprint		<b>3. DATES COVERED (From - To)</b> 30 April 2004 – 01 December 2006			
<b>4. TITLE AND SUBTITLE</b> MEASUREMENTS OF NO AND OH CONCENTRATIONS IN VITIATED AIR USING DIODE LASER-BASED ULTRAVIOLET ABSORPTION SENSORS (POSTPRINT)				<b>5a. CONTRACT NUMBER</b> In-house			
				<b>5b. GRANT NUMBER</b>			
				<b>5c. PROGRAM ELEMENT NUMBER</b> 61102F			
<b>6. AUTHOR(S)</b> Thomas N. Anderson and Robert P. Lucht (Purdue University) Terrence R. Meyer, Tarun Mathur, and Keith D. Grinstead, Jr. (Innovative Scientific Solutions, Inc.) James R. Gord, Mark Gruber, and Campbell D. Carter (AFRL/RZAS)				<b>5d. PROJECT NUMBER</b> 2308			
				<b>5e. TASK NUMBER</b> AI			
				<b>5f. WORK UNIT NUMBER</b> 2308AI00			
<b>7. PERFORMING ORGANIZATION NAME(S) AND ADDRESS(ES)</b> <table style="width: 100%; border: none;"> <tr> <td style="width: 50%; border-right: 1px solid black; padding: 5px; vertical-align: top;">           Purdue University            West Lafayette, IN 47907            -----            Innovative Scientific Solutions, Inc.            Dayton, OH 45440         </td> <td style="width: 50%; padding: 5px; vertical-align: top;">           Propulsion Sciences Branch (AFRL/RZAS)            Aerospace Propulsion Division            Air Force Research Laboratory, Propulsion Directorate            Wright-Patterson Air Force Base, OH 45433-7251            Air Force Materiel Command, United States Air Force         </td> </tr> </table>				Purdue University West Lafayette, IN 47907 ----- Innovative Scientific Solutions, Inc. Dayton, OH 45440	Propulsion Sciences Branch (AFRL/RZAS) Aerospace Propulsion Division Air Force Research Laboratory, Propulsion Directorate Wright-Patterson Air Force Base, OH 45433-7251 Air Force Materiel Command, United States Air Force	<b>8. PERFORMING ORGANIZATION REPORT NUMBER</b> AFRL-RZ-WP-TP-2008-2032	
Purdue University West Lafayette, IN 47907 ----- Innovative Scientific Solutions, Inc. Dayton, OH 45440	Propulsion Sciences Branch (AFRL/RZAS) Aerospace Propulsion Division Air Force Research Laboratory, Propulsion Directorate Wright-Patterson Air Force Base, OH 45433-7251 Air Force Materiel Command, United States Air Force						
<b>9. SPONSORING/MONITORING AGENCY NAME(S) AND ADDRESS(ES)</b> Air Force Research Laboratory Propulsion Directorate Wright-Patterson Air Force Base, OH 45433-7251 Air Force Materiel Command United States Air Force				<b>10. SPONSORING/MONITORING AGENCY ACRONYM(S)</b> AFRL/RZAS			
				<b>11. SPONSORING/MONITORING AGENCY REPORT NUMBER(S)</b> AFRL-RZ-WP-TP-2008-2032			
<b>12. DISTRIBUTION/AVAILABILITY STATEMENT</b> Approved for public release; distribution unlimited.							
<b>13. SUPPLEMENTARY NOTES</b> Conference paper published in the Proceedings of the 45th AIAA Aerospace Sciences Meeting and Exhibit. © 2007 American Institute of Aeronautics and Astronautics, Inc. The U.S. Government is joint author of the work and has the right to use, modify, reproduce, release, perform, display, or disclose the work. Technical paper contains color. PAO Case Number: AFRL/WS 06-2905, 27 Dec. 2006.							
<b>14. ABSTRACT</b> Diode-laser-based sensors were implemented to measure the concentrations of nitric oxide (NO) and hydroxyl (OH) radicals in the vitiated inlet airflow of a model scramjet combustor. The sensors utilized sum-frequency-mixed sources consisting of a fixed frequency 532-nm laser and a tunable diode laser to generate ultraviolet radiation for absorption spectroscopy with electronic transitions of OH and NO. Sensitive, interference-free, absolute measurements were possible, enabling the first measurements of both species in a model scramjet combustor using diode-laser-based sensors. With wavelength-modulation spectroscopy, no absorption by OH was evident in the vitiated airflow, verifying that the OH concentration was below the 0.2-ppm detection limit of the sensor.							
<b>15. SUBJECT TERMS</b>							
<b>16. SECURITY CLASSIFICATION OF:</b>			<b>17. LIMITATION OF ABSTRACT:</b> SAR	<b>18. NUMBER OF PAGES</b> 18	<b>19a. NAME OF RESPONSIBLE PERSON (Monitor)</b> Campbell D. Carter <b>19b. TELEPHONE NUMBER (Include Area Code)</b> N/A		
<b>a. REPORT</b> Unclassified	<b>b. ABSTRACT</b> Unclassified	<b>c. THIS PAGE</b> Unclassified					

# Measurements of NO and OH Concentrations in Vitiated Air Using Diode-Laser-Based Ultraviolet Absorption Sensors

Thomas N. Anderson<sup>1</sup> and Robert P. Lucht<sup>2</sup>  
*Purdue University, West Lafayette, Indiana 47907*

Terrence R. Meyer<sup>3</sup>, Tarun Mathur,<sup>4</sup> and Keith D. Grinstead, Jr.<sup>5</sup>  
*Innovative Scientific Solutions, Inc., Dayton, Ohio 45440*

and

James R. Gord<sup>6</sup>, Mark Gruber<sup>7</sup>, and Campbell D. Carter<sup>8</sup>  
*Air Force Research Laboratory, Propulsion Directorate, Wright-Patterson AFB, Ohio 45433*

Diode-laser-based sensors were implemented to measure the concentrations of nitric oxide (NO) and hydroxyl (OH) radicals in the vitiated inlet airflow of a model scramjet combustor. The sensors utilized sum-frequency-mixed sources consisting of a fixed-frequency 532-nm laser and a tunable diode laser to generate ultraviolet radiation for absorption spectroscopy with electronic transitions of OH and NO. Sensitive, interference-free, absolute measurements were possible, enabling the first measurements of both species in a model scramjet combustor using diode-laser-based sensors. With wavelength-modulation spectroscopy, no absorption by OH was evident in the vitiated airflow, verifying that the OH concentration was below the 0.2-ppm detection limit of the sensor. Concentrations of NO were measured to be 200-1100 ppm for the vitiator conditions tested.

## Nomenclature

$A$	=	nozzle area
$A^*$	=	nozzle area at throat
$M$	=	Mach number
$p$	=	static pressure
$p_0$	=	stagnation pressure
$T$	=	static temperature
$T_0$	=	stagnation temperature
$x$	=	position along flow direction
$k$	=	specific heat ratio

## I. Introduction

VITIATION has long been used to simulate high-Mach number flight conditions for ground tests of supersonic propulsion systems. In the vitiation process, air is heated to flight conditions by combusting fuel with air and adding oxygen to maintain the oxygen content of normal air. Many parameters of flight air can be closely simulated with the vitiated air such as Mach number, total enthalpy, oxygen content, and stagnation temperature. In addition,

<sup>1</sup> Research Assistant, School of Mechanical Engineering, 585 Purdue Mall, MS 1288, and AIAA Student Member.

<sup>2</sup> Professor, School of Mechanical Engineering, 585 Purdue Mall, MS 1288, and AIAA Associate Fellow.

<sup>3</sup> Assistant Professor, Dept. of Mechanical Engineering, Iowa State Univ., Ames, Iowa; AIAA Associate Fellow.

<sup>4</sup> Research Engineer; AIAA Senior Member.

<sup>5</sup> Research Chemist; AIAA Member.

<sup>6</sup> Principal Research Chemist; AIAA Associate Fellow.

<sup>7</sup> Senior Aerospace Engineer; AIAA Associate Fellow.

<sup>8</sup> Senior Aerospace Engineer; AIAA Associate Fellow.

vitiation is easier, less expensive, and more efficient than other heating techniques such as arc heating and thermal storage. However, the combustion process in the vitiator alters the composition of the air, adding  $\text{H}_2\text{O}$ ,  $\text{CO}_2$ , OH, NO, and CO.

Many studies have demonstrated that these “contaminants” in vitiated air can significantly affect combustion behavior. For example, several groups have demonstrated accelerated ignition in supersonic combustion in the presence of small levels of OH,<sup>1,2</sup> NO,<sup>2-5</sup> and other species.<sup>7-9</sup> It is likely that these contaminants also affect other combustion parameters such as flame holding or stability, although no studies are available to verify these effects. If the composition of vitiated air is significantly different than that of normal air experienced in flight, then the results of supersonic ground tests might not be valid for actual flight conditions.

In order to assess the impact of contaminants from vitiation, the actual composition of vitiated air must first be measured. Optical sensors provide a convenient, non-intrusive means for measuring the concentration of the various contaminants. In particular, diode-laser-based sensors are rugged enough to survive the harsh environments of many supersonic combustion test cells, and these sensors provide absolute measurements of species concentration.

Water vapor is the most readily accessible molecule to study with diode-laser-based sensors because of the many water vapor transitions that coincide with telecommunications lasers. Three separate groups have previously used diode-laser-based sensors to measure water vapor concentration and temperature in model scramjet combustors.<sup>9-11</sup> All three previous measurements demonstrated that diode-laser-based sensors can be employed in model scramjet combustors if sufficient care is taken to mitigate beam-steering effects from the high-speed flow. Nitric oxide (NO) has also been measured in a hypersonic wind tunnel using a cryogenically-cooled lead-salt diode laser.<sup>12</sup> However, these previous NO measurements were severely affected by boundary layers around the supersonic flow, and the NO mole fraction measurements were only accurate to within an order of magnitude due to noise. No measurements of hydroxyl (OH) radical concentration have been demonstrated in vitiated air with a diode-laser-based sensor.

In the experiments described in this paper, we have used diode-laser-based sensors to measure NO and OH concentrations in the vitiated inlet air of a model scramjet combustor at Wright-Patterson Air Force Base in Dayton, Ohio. By employing newly developed diode-laser-based sensors that allow us to probe strong electronic transitions of NO and OH in the ultraviolet (UV) spectral region,<sup>13-16</sup> we were able to quantify the concentrations of both molecules in the vitiated air. To the authors’ knowledge, these experiments represent the first reported measurements of NO and OH in vitiated air using diode-laser-based sensors. Quantitative measurements of both these species provide much-needed information on the composition of the vitiated airflow to determine the actual effects on combustion in the model scramjet combustor.

## II. Scramjet Facility

The model scramjet combustor facility at Wright-Patterson AFB is used to study supersonic fuel injection, flameholding, ignition, and inlet-combustor isolation in scramjet propulsion systems.<sup>17</sup> A diagram of the scramjet facility is shown in Figure 1. Details of the facility can be found in Gruber *et al.*<sup>17</sup> and Mathur *et al.*<sup>18</sup> and references therein. A continuous flow of preheated air at 13.6 kg/s, 5.2 MPa, and 920 K is supplied by the Research Air Facility at Wright-Patterson AFB. The supply air is heated further in a sudden expansion vitiator that was fueled with natural gas. Make-up oxygen is added to the vitiated air to replenish the oxygen burned during combustion in the vitiator. The stagnation temperature and pressure of the vitiated air is measured with probes in the water-cooled instrumentation section just downstream of the vitiator. The high-temperature, high-pressure air is then compressed from axisymmetric (254-mm diameter) to two-dimensional (57.2 x 177.8 mm) before being expanded through the facility nozzle to Mach 2.5.

After the expansion, the vitiated airflow passes through two isolator sections to contain the pre-combustion pressure rise before entering the model scramjet combustor. The combustor section has fused-silica windows to allow optical access for the diode-laser-based sensor measurements, as shown in the photograph in Figure 1. Optics for the sensor measurements were mounted on optical breadboards mounted beside the windows. The layout of the optics at the combustor section is described in the next section.

After the combustor section, the airflow is routed through a calorimeter and then out of the test cell through an exhaustor. The composition of the vitiated airflow was monitored throughout the tests with a commercial gas analyzer (ECOM America, Ltd.), and air was sampled from a probe located at the exit of the combustor section. The static pressure along the flow path in the combustor section was measured with pressure taps. Flow section areas were also known at every point along the flow path in the combustor section. Using either the static pressures or the flow section areas along with the stagnation conditions at the combustor inlet, the Mach numbers at the measurement locations were calculated for analysis of the diode-laser-based sensor data. The calculations are discussed in Section IV.

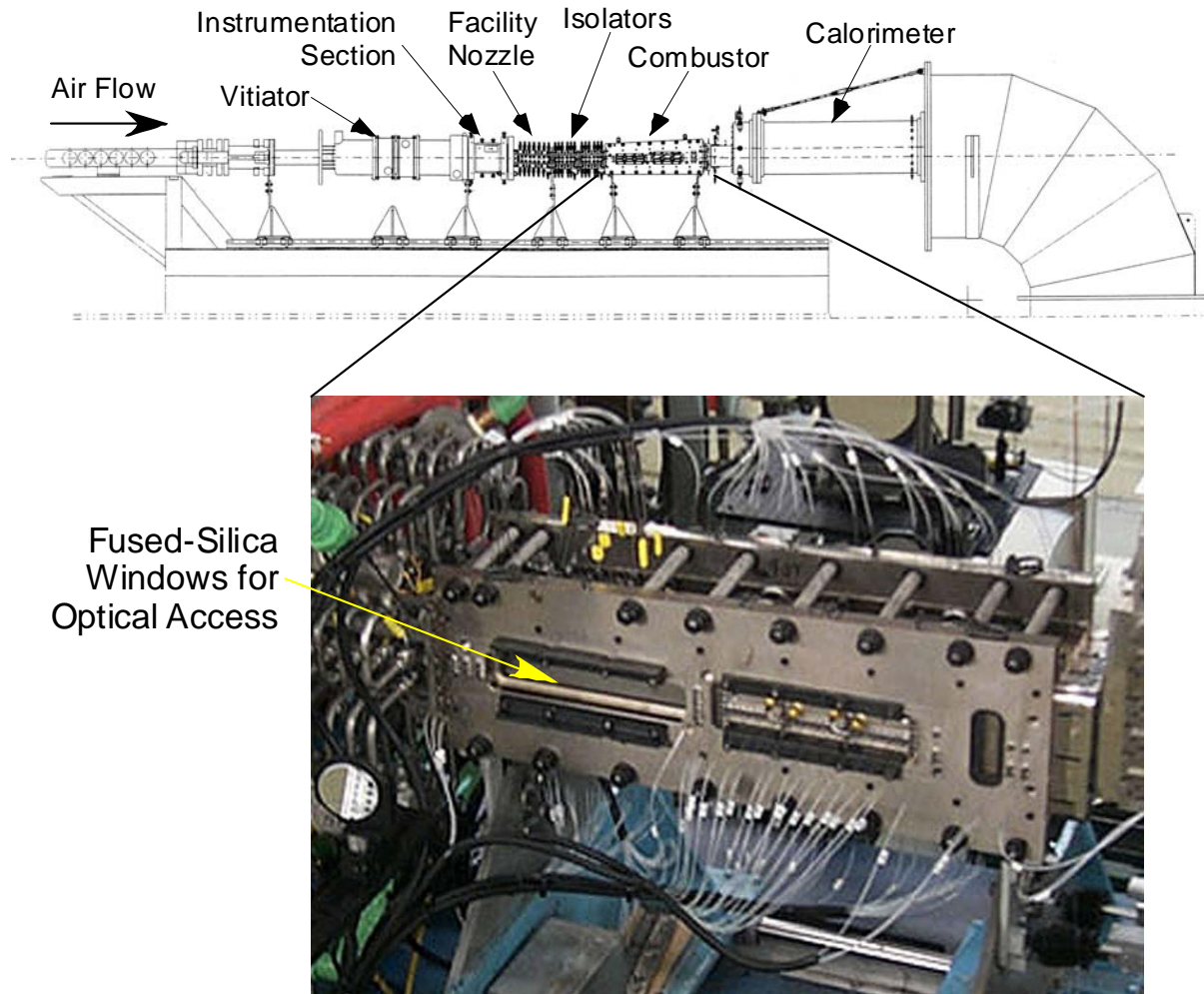


**Figure 1. Schematic diagram of the scramjet facility at Wright-Patterson Air Force Base in Dayton, Ohio, and a photograph of the combustor section where OH and NO measurements were performed.**

### III. Diode-Laser-Based Sensor Systems

The two diode-laser-based sensors used to measure NO and OH in the scramjet have been previously developed and demonstrated.<sup>13-16</sup> Detailed descriptions of the sensors are available in Refs. 13-16, but the general layout of each sensor is briefly discussed here along with the modifications required for measurements in the scramjet facility. Both sensors utilize sum-frequency mixing to generate tunable UV radiation that is used to perform absorption spectroscopy of OH and NO. They utilize a common architecture in which a high-power, fixed-frequency, 532-nm laser is mixed with a tunable diode laser in a beta-barium borate ( $\beta$ -BBO) crystal. For performing absorption spectroscopy, part of the generated UV radiation is measured immediately as a reference and the remainder is coupled into an optical fiber to simplify the transmission of the beam through the scramjet combustor.

#### A. OH Sensor

In the OH sensor, around 35 mW of 763-nm radiation from a rapidly-tunable distributed feedback (DFB) diode laser (Sacher Lasertechnik) is mixed with 5 W of 532-nm radiation from a frequency-doubled, Nd:YVO<sub>4</sub> laser (Coherent Verdi). A schematic diagram of the system is shown in Figure 2. Typically, around 25  $\mu$ W of UV is generated at a wavelength of 313.5 nm, which is in resonance with the (0,0) band of the  $A^2\Sigma^+-X^2\Pi$  electronic

transition of OH. The UV is separated from the fundamental beams using two mirrors HR-coated for 310 nm, and then split with a 70/30 beamsplitter. The 30% reflected is sent directly through a colored-glass filter (UG-11; 3-mm thick) and onto a UV-enhanced Si photodiode (Advanced Photonix) to provide the reference intensity as the laser is current tuned. The remaining 70% of the UV radiation transmitted through the beamsplitter is reflected once more with a 310-nm mirror and then coupled into a 2-m-long, 600- $\mu\text{m}$ -core-diameter, fused silica optical fiber (Ocean Optics; P600-2-UV/VIS). The entire optical system was built on a 61-cm x 61-cm breadboard.

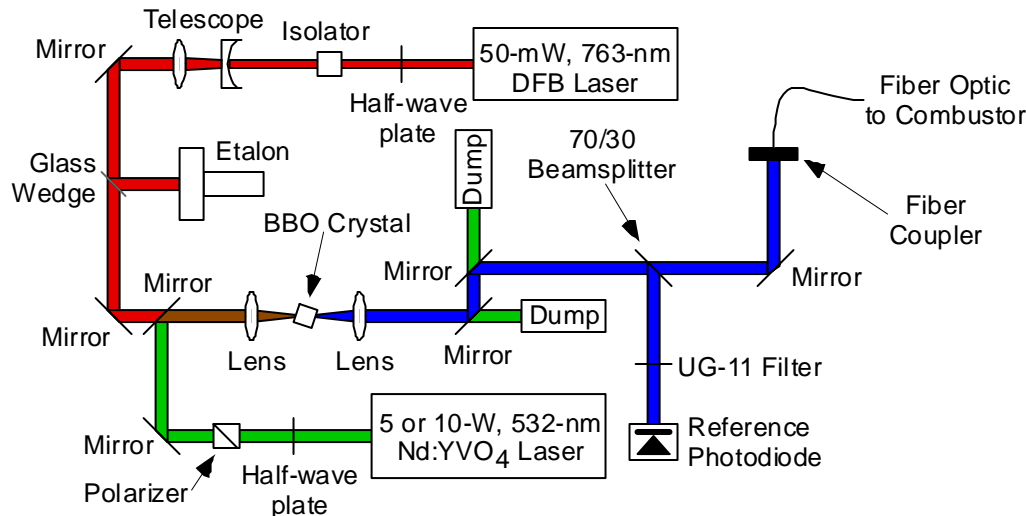


**Figure 2. Schematic diagram of the diode-laser-based sensor used to measure OH concentration.**

At the combustor section, the UV beams for both OH and NO measurements were directed as shown in Figure 3. For the OH sensor, the 313.5-nm radiation in the fiber was sent to an optical breadboard mounted beside the scramjet combustor section. The laser system was placed on a cart away from the combustor to reduce vibrations and to maintain a stable operating temperature. At the test section, the UV beam exited the fiber through a fused-silica fiber coupler mounted in a 6-axis mount. An  $f=75\text{-mm}$  lens was placed approximately 75 mm from the end of the fiber coupler to collimate the UV beam as it passed through the combustor. The beam diameter on the windows was roughly 2.2 cm. The UV beam was located approximately 32 cm downstream from the nozzle exit. After passing through the fused-silica windows, the beam was reflected back through the 22.86-cm-wide

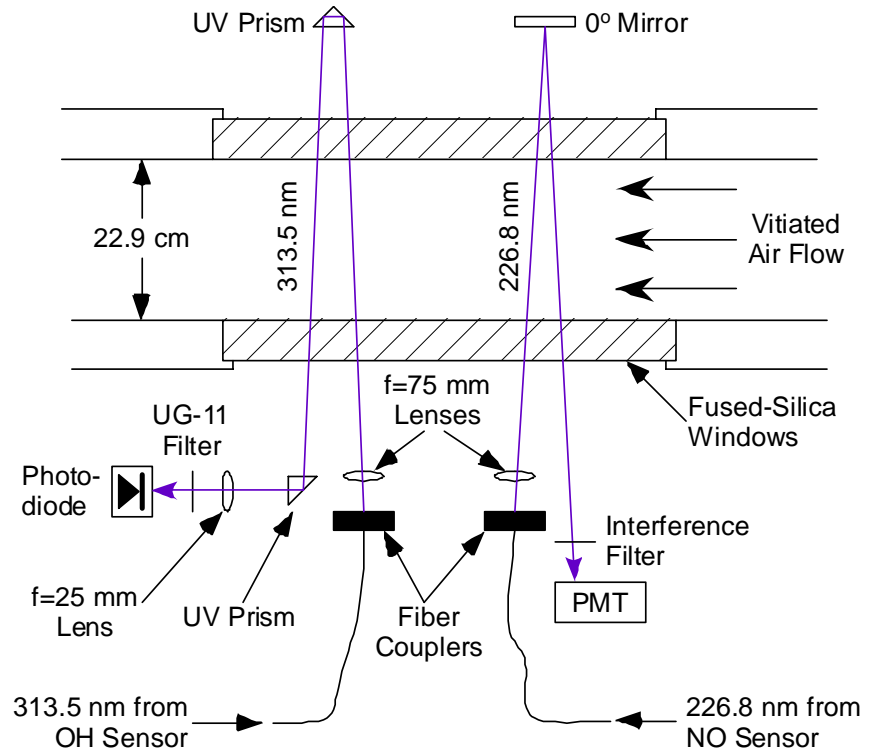


**Figure 3. Schematic diagram of the optical layout in the scramjet combustor for measurements of OH and NO with diode-laser-based sensors.**

combustor using a 2.54-cm x 2.54-cm fused-silica prism that was AR-coated for 248-355 nm. A second prism was used to direct the beam to an  $f=25$ -mm lens to focus the beam onto the photodetector. A 3-mm-thick UG-11 filter was placed before the photodetector to block the fundamental laser radiation and room light. The remainder of the optics in the OH sensor were the same as for the previous configuration described in Meyer *et al.* and Anderson *et al.*<sup>15,16</sup> It should be noted that the beamsplitter and reference detector were still in place to attempt direct absorption measurements in addition to WMS measurements.

Control and modulation of the OH sensor were performed remotely from inside the control room. The data acquisition computer was located in the research cell next to the sensors, and the computer was controlled remotely with a PC extender. Second-harmonic detection with wavelength-modulation spectroscopy (2f WMS) was used, and the 2f-WMS lineshapes were acquired and processed as described in Anderson.<sup>20</sup> The DFB laser was modulated with a signal composed of a 50-kHz sine wave (0.42-V amplitude) added to a 10-Hz triangle-wave function (0.7-V amplitude). The photodiode signal was demodulated through the lock-in amplifier (Stanford Research Systems, SR850) and recorded with the computer. All spectra were averaged over 100 complete cycles of the triangle-wave function to decrease the noise. The lock-in amplifier settings were the following: 300  $\mu$ s time constant, 500  $\mu$ V sensitivity, 24 dB/oct filter slope, 143.8° phase angle, and maximum dynamic reserve. The 300- $\mu$ s time constant represents a filter bandwidth of 260 Hz, and when averaged over 100 sweeps, the final detection bandwidth is 2.6 Hz.

## B. NO Sensor

For the NO sensor, the tunable laser is an external cavity diode laser (ECDL) at 395-nm (Toptica Photonics), as shown in Figure 4. Around 11 mW of radiation from this laser is mixed with 100 mW of 532-nm radiation from a diode-pumped, intracavity-frequency-doubled Nd:YAG laser (CrystalLaser). Approximately 325 nW of UV is generated at 226.8 nm to probe transitions in the (0,0) band of the  $A^2\Sigma-X^2\Pi$  electronic transition of NO. The UV is recollimated after the crystal and then split with a 50/50 beamsplitter. The reflected beam is used as a reference and is sent through two interference filters centered at 228 nm (Andover) and onto a solar-blind photomultiplier tube (PMT; Hamamatsu, R7154). Two filters were required to adequately block the 395-nm radiation since the PMT is relatively sensitive to radiation at this wavelength. The transmitted beam is fiber coupled into a 2-m-long, 600- $\mu$ m-core-diameter, fused silica optical fiber (Ocean Optics; P600-2-UV/VIS) to send to the test section. This entire optical system was built on a 45.7-cm x 45.7-cm breadboard, which is substantially smaller than the 61-cm x 122-cm breadboard used previously for this sensor.<sup>14</sup> The smaller packaging facilitated transport of the sensor and simplified the setup near the scramjet facility since the breadboard could be placed on the same table with the OH sensor.

NO sensor measurements were performed using direct absorption spectroscopy where the wavelength of the UV radiation was slowly tuned over the transition by changing the angle of the diffraction grating in the ECDL. A

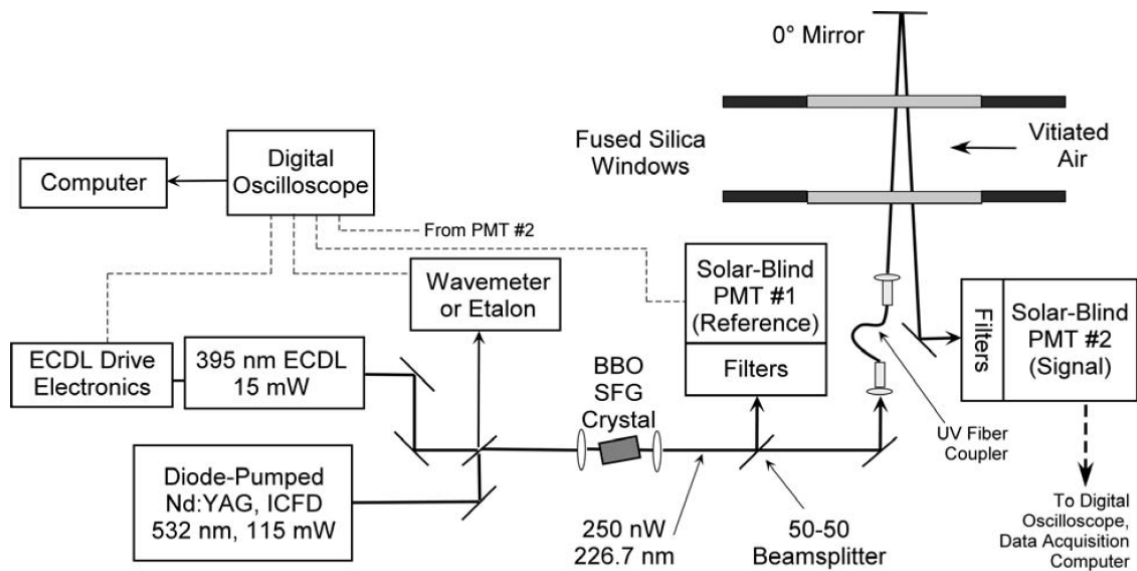


**Figure 4. Schematic diagram of NO sensor system for scramjet experiments.**

simultaneous correction of the injection current was also required to prevent mode hops during tuning. A 20-Hz triangle-wave function was output from the AI/AO card, and the voltage was doubled with a 2x amplifier to an amplitude of 15 V; this voltage was applied directly to the laser head to modulate the piezoelectric crystal that moves the diffraction grating. A second triangle-wave function with an amplitude of 0.165 V was generated with the AI/AO card and applied to the ECDL controller to modulate the injection current of the laser. With this configuration, a 15 GHz mode-hop-free tuning range was achieved. A larger tuning range could be achieved if a larger amplifier were available to overcome the  $\pm 10$  V limitation of the AI/AO card. Further details of the wavelength scanning technique are discussed in Anderson *et al.*<sup>19</sup>

The optical layout for the NO sensor at the combustor section is shown in Figure 3. UV radiation at 226.8 nm from the optical fiber was pitched across the combustor test section with a fused-silica fiber coupler mounted on a 6-axis mount. All optics were attached to a breadboard mounted next to the scramjet combustor. The NO sensor was placed on a table several feet away from the flow facility to shield the sensor from vibrations and high temperatures. Like the OH sensor, an  $f=75$ -mm fused-silica lens was used to collimate the light from the coupler to maintain a constant beam diameter of roughly 3 cm throughout the two passes through the combustor. A  $0^\circ$  mirror for 226 nm was used on the opposite side of the combustor to reflect the UV beam back through the combustor and onto the PMT. Two narrowband interference filters (Andover 228FS10-25) were placed before the PMT to block the fundamental radiation and room lights. The UV beam for the NO sensor measurements was located approximately 21.9 cm downstream of the facility isolator exit.

As with the OH sensor, the NO sensor was controlled remotely from a computer inside the control room. The computer with the DAQ system was placed next to the sensor and controlled from inside the control room using a PC extender. This allowed us to use short BNC cables for control and acquisition with the sensor. The ECDL was controlled using the two-signal scheme described above to achieve a mode-hop-free tuning range of 15 GHz. An etalon was also simultaneously recorded to monitor the frequency change of the ECDL during the scans. The laser was scanned at 20 Hz and 100 scans were averaged to reduce noise. Photocurrents from the PMTs were detected across 50-k $\Omega$  resistors and filtered with the filter/preamplifiers using a cutoff frequency of 1 kHz and amplified with a gain of 5x on the signal PMT voltage and 50x on the reference PMT voltage. Detector and etalon signals were recorded using the DAQ system and processed according to the procedure described in Anderson *et al.*<sup>14</sup> Fuel flow for the vitiator was cut off between every other condition to record air scans to be used in the normalization. The ECDL wavelength was adjusted to 395.2819 nm to probe the  $P_2(9)$  transition (for NO) at 44084.69  $\text{cm}^{-1}$ .

## IV. Results

### A. OH Measurements

The 2f-WMS data were recorded in the vitiated air for vitiator temperatures from 1000 to 1389 K. The averaged raw 2f-WMS signal recorded at the scramjet combustor for a vitiator temperature of 1389 K is shown in Figure 5. The averaged raw 2f-WMS signal acquired in hot air immediately after shutting off the vitiator is also shown in Figure 5. Taking the difference of the two scans, it is evident that there is no absorption by OH in the vitiated air. The 2f-WMS feature resulting from absorption of the 763-nm beam by oxygen provides a convenient frequency reference to ensure that the UV wavelength is correct. Using this frequency reference, a theoretical OH 2f-WMS lineshape was generated and compared with the corrected experimental 2f-WMS signal in Figure 6.

The theoretical 2f-WMS lineshape in Figure 6 was calculated for 1 ppm of OH at the measured pressure and calculated temperature (see Section IV.B for temperature calculations) at the beam location inside the scramjet combustor test section. The collision width was estimated for air at the measured temperature. All parameters used in the theoretical calculation are included in Figure 6. The three parameters for the WMS lineshape were calculated from calibration of the sensor based on a modulation voltage amplitude of 0.42 V. Details of the calibration are available in Anderson.<sup>20</sup>

From Figure 6, it is clear that there is no detectable absorption by OH in the vitiated air, even at the highest vitiator temperature. Therefore, the OH mole fraction is below the detection limit of the OH sensor in the current configuration. To estimate the detection limit, the peak 2f-WMS signal for 1 ppm is noted to be 0.43 V from Figure 6 for the 0.457-m path length through the test section. The noise in the corrected 2f-WMS spectrum in Figure 6 has a standard deviation of approximately 0.1 V. Thus, the detection limit (for SNR=1) of the OH sensor is  $\sim 0.2$  ppm for the path length and conditions in the scramjet combustor test section. For comparison with the detection limit in previous configurations, this corresponds to a detection limit of 0.1 ppm-m OH in 700-K gas at a 0.1-Hz rate. In a 10-second averaging time, the detection limit for the WMS configuration during laboratory experiments was 0.04 ppm-m.<sup>20</sup>



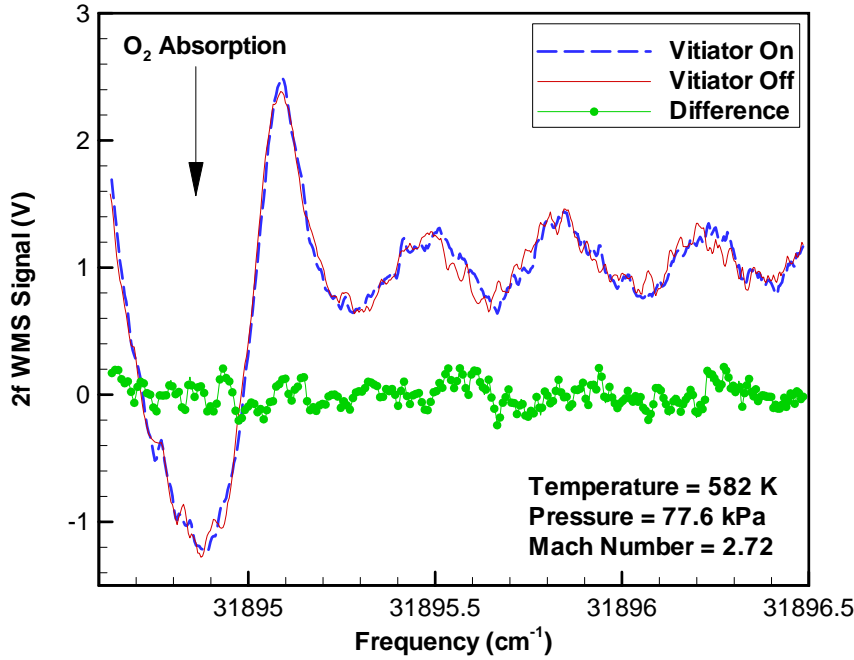


Figure 5. Raw 2f-WMS signals acquired with the OH sensor with the vitiator on and off and the difference of the two signals for a vitiator stagnation temperature of 1389 K. The static temperature, static pressure, and Mach number at the measurement location are shown. The 2f-WMS signal resulting from absorption of the 763-nm beam by oxygen before the crystal is indicated.

For vitiator stagnation temperatures of 1000 K to 1389 K, no OH was observed in the vitiated air with the OH sensor. Thus, we have demonstrated that the OH levels in the vitiated airflow at the combustor test section in the scramjet facility are below 0.2 ppm. Most numerical studies have shown that much greater levels of OH than these are required to significantly affect ignition chemistry in supersonic combustors.<sup>1,2</sup> Therefore, our measurements indicate that vitiator-generated OH should not affect the results of ground tests using the scramjet facility. This proof that OH is negligible in the vitiated airflow increases the confidence in past and future results with the model scramjet combustor at Wright-Patterson Air Force Base.

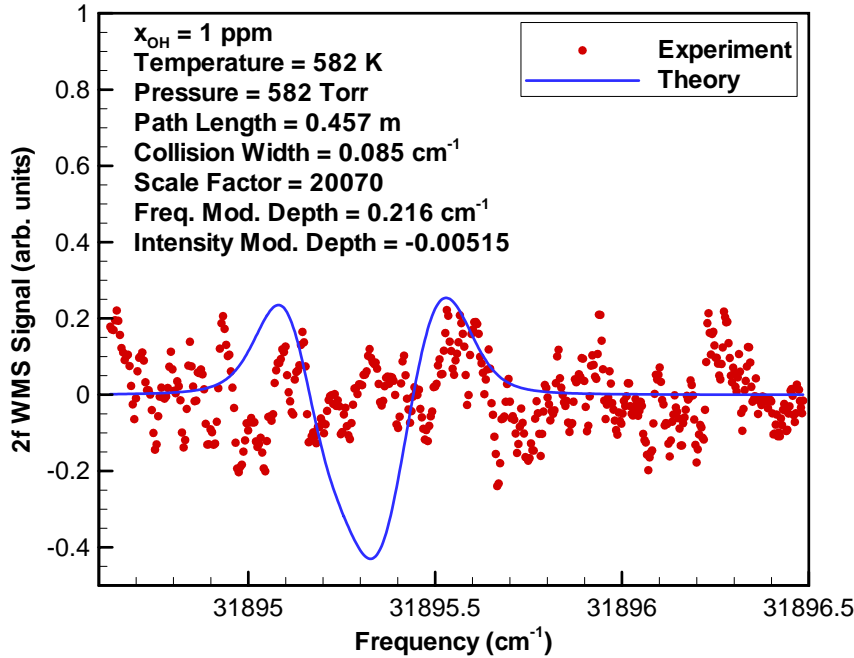


Figure 6. Corrected 2f-WMS signal (difference from Figure 5) and theoretical 2f-WMS signal for 1 ppm of OH at the conditions for the scan in Figure 5.

## B. NO Measurements

Five different vitiator conditions were tested during the scramjet experiments so that the stagnation temperatures at the vitiator exit ranged from 1000 K to 1389 K. The static temperature, pressure, and Mach number of the air at the location of the 226-nm beam in the combustor section are shown in Table 1 for each vitiator condition. Pressure taps were located along the length of the combustor section to directly measure the static pressure at the beam location, and the pressures reported in Table 1 are single-shot measurements at each condition. No thermocouples were placed in the combustor test section, however, and two different methods were used to estimate the static temperature at the 226-nm beam location. In Method A, we used the static pressure to estimate the static temperature,  $T$ , at the beam location with the equation<sup>21</sup>

$$T = T_0 \left( \frac{p}{p_0} \right)^{(k-1)/k},$$

where  $T_0$  is the stagnation temperature at the facility-nozzle exit,  $p$  is the static pressure at the NO beam location,  $p_0$  is the stagnation pressure at the vitiator exit, and  $k$  is the specific heat ratio. In Method B, we used the area ratio between the nozzle area at the beam location [ $A(x)$ ] and the nozzle area at the throat ( $A^*$ ) to calculate the Mach number by iterating the equation<sup>21</sup>

$$\frac{A(x)}{A^*} = \frac{1}{M} \left[ \frac{1 + \frac{k-1}{2} M^2}{1 + \frac{k-1}{2}} \right]^{(k+1)/2(k-1)},$$

where  $M$  is the Mach number at the beam location. Using the calculated Mach number at the beam location, the local static temperature is calculated using

$$T = T_0 \left[ 1 + \frac{k-1}{2} M^2 \right]^{-1}.$$

The temperatures calculated using each method are within 5% of each other, as listed in Table 1. NO mole fractions were calculated using both temperatures to investigate the influence of temperature. However, the temperatures calculated using Method B were assumed to be more accurate since the flow section areas were known precisely whereas the measured static pressures used in Method A were only single-shot measurements and therefore were susceptible to larger fluctuations.

Absorption spectra of NO in the vitiated air for two vitiator stagnation temperatures are shown in Figure 7. The theoretical lineshapes for these and all spectra in the scramjet experiments were calculated by fixing the temperature and pressure to the values from Table 1. The transmission scale factor was also fixed to unity since no broadband attenuation was observed in the signals. Only the NO mole fraction and collision width were allowed to vary to optimize the fit. At the lowest two vitiator temperatures, the theoretical lineshapes agree closely with the

**Table 1. Conditions of the vitiated airflow in the model scramjet combustor at the location of the 226-nm beam for NO measurements for the vitiator stagnation temperatures tested.**

Vitator Stagnation Temp. (K)	Static Temp. at Test Location (K) <sup>a</sup>	Static Temp. at Test Location (K) <sup>b</sup>	Static Pressure at Location (kPa)	Mach Number at Test Location
1000	410	390	62.0	2.61
1111	466	436	64.8	2.58
1222	526	496	65.0	2.58
1333	593	559	66.2	2.57
1389	619	587	65.9	2.57

<sup>a</sup>Calculated using the static pressure measured at the beam location

<sup>b</sup>Calculated using the flow-section area at the beam location.

experimental lineshapes, as demonstrated in Figure 7(a). Unfortunately, the agreement between theoretical and experimental absorption lineshapes worsens as the vitiator temperature increases. The spectra from the highest three vitiator temperatures become asymmetric on the low-frequency side, as illustrated in the spectrum in Figure 7(b) for the highest vitiator temperature. On the high-frequency side of the spectra, the experimental and theoretical

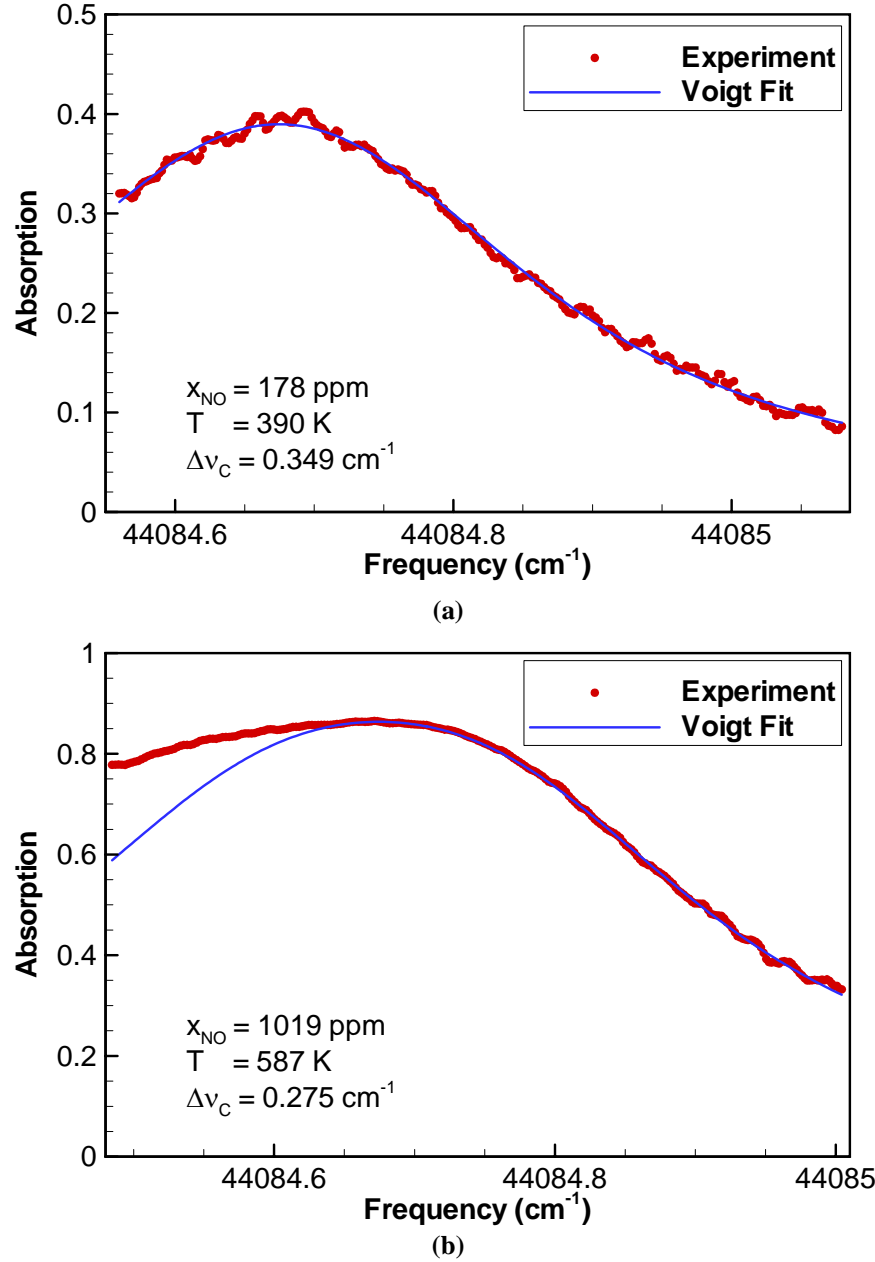


**Figure 7. Averaged absorption spectra acquired with the NO sensor in the vitiated airflow for the scramjet combustor for vitiator stagnation temperatures of a) 1000 K and b) 1389 K. Both spectra were acquired in 2.5 seconds (40 Hz, 100 sweeps averaged).**

each condition. Collision-broadening coefficients for NO broadened by  $N_2$  and  $O_2$  were calculated using expressions from Chang *et al.*<sup>22</sup> and DiRosa *et al.*,<sup>23</sup> and the total collision width was summed according to expressions in the references. The calculated collision widths for NO in air (79%  $N_2$  and 21%  $O_2$  by volume) were

absorption lineshapes agree closely, and reasonable values of NO mole fraction and collision width can be extracted from the fit to only the high-frequency portion of the lineshapes.

The NO mole fractions determined from the spectral fits at each condition are shown in Figure 8. Gas temperatures calculated using the area ratios (Method B) were used for the results in Figure 8. The temperatures calculated using Method A resulted in NO mole fractions that were 6-9% higher than those in Figure 8. As mentioned earlier, the temperatures (and therefore NO mole fractions) determined using Method B are believed to be most accurate, so the NO mole fractions in Figure 8 represent the most accurate measurement of NO at each vitiator temperature. As seen in Figure 8, the diode-laser-based sensor measurements of NO agree closely with measurements from the ECOM analyzer for lower vitiator temperatures. At higher temperatures, we believe that the diode-laser-sensor measurements are not as sensitive because the UV beam is almost completely attenuated after two passes through the vitiated air stream. Future tests are planned with only a single pass through the combustor to re-examine the high-temperature conditions.

In addition to NO mole fractions, we also compare the observed collision widths to calculations for air at the pressure and temperature for

consistently around 20% smaller than the actual collision widths. The reason for the discrepancy in collision widths is unknown at this time.

Another phenomenon was also observed in the NO spectra acquired in the vitiated airflow. As seen in the experimental absorption spectra in Figure 9, there is a shift in the line center to higher frequencies as the vitiator temperature increases. In this figure, the absorption lineshape for the 1000-K case was shifted to the actual line center frequency ( $44084.69 \text{ cm}^{-1}$ ), and all the remaining spectra were shifted by the same amount to illustrate the magnitude of the frequency shift. By comparing the etalon fringes for each case, a shift of only  $0.013 \text{ cm}^{-1}$  was observed in the laser frequency between the lowest and highest vitiator temperatures. The observed frequency difference between line center of the 1000-K and 1389-K spectra is  $\sim 0.08 \text{ cm}^{-1}$ . Thus, the actual shift in line center frequency is approximately  $0.07 \text{ cm}^{-1}$  between the lowest and highest vitiator temperature spectra.

At present, neither the asymmetry nor the excessive collision widths can be readily explained. The effects of potential boundary layers in the flow were investigated, but even severe gradients in pressure, velocity, and temperature did not cause significant broadening or shift in simulated path-averaged spectra. Previous studies of temperature and pressure gradients in the scramjet combustor have shown relatively uniform profiles.<sup>17</sup> Another

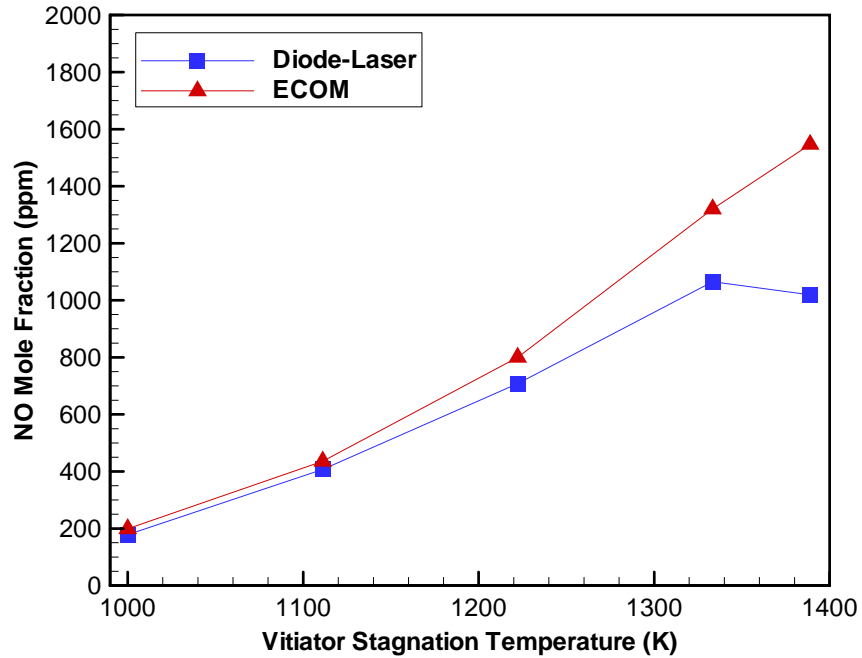


**Figure 8. Variation of measured NO mole fractions with vitiator stagnation temperature as measured with the diode-laser sensor and commercial gas analyzer (ECOM).**

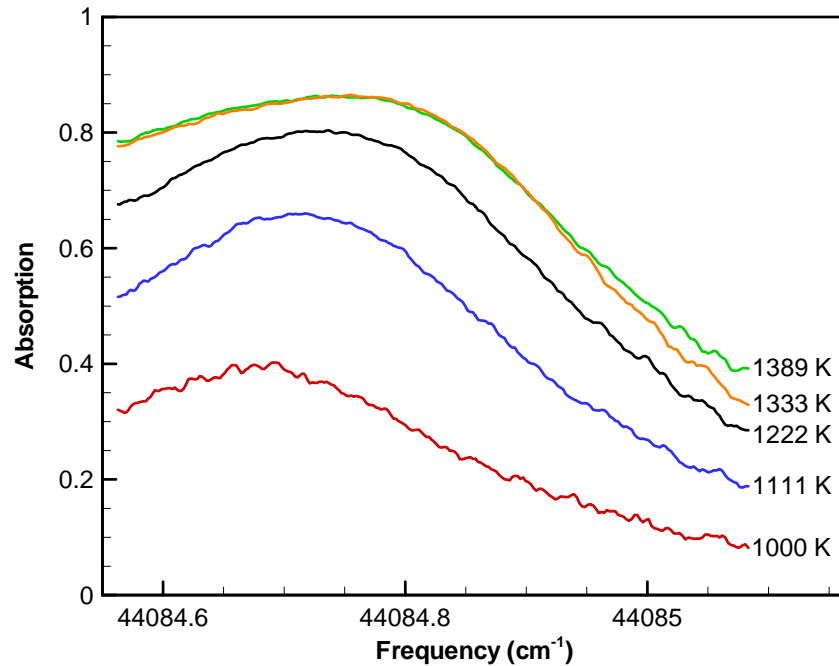


**Figure 9. Averaged experimental absorption spectra for all conditions tested in the scramjet experiments. The spectrum for the 1000 K case was shifted to the correct absolute frequency, and the remaining spectra were shifted by the same amount to show the line shift with increasing vitiator temperature.**

possibility is absorption by an interfering species. However, most species that are present in appreciable amounts in the vitiated air display only broadband absorption in this spectral region. No transmission scale was necessary in the spectral fits to the NO absorption data, so this possibility is not likely either. Further experiments are planned to investigate the causes of these phenomena.

Nonetheless, the NO mole fractions measured with the diode-laser sensor provide reasonable estimates for the NO contamination in the vitiated airflow for each vitiator condition. Using these data, researchers using the scramjet combustor at Wright-Patterson AFB can begin to calculate the effect on future hypersonic combustion experiments in the facility.

## V. Conclusion

Measurements of both OH and NO concentrations have been performed using newly developed diode-laser-based sensors. The sensors are based on sum-frequency-mixing of a high-power, fixed-frequency, 532-nm laser with a tunable diode laser in a BBO crystal. The resulting UV radiation is in resonance with electronic transitions of NO or OH to perform absorption spectroscopy with little interference from other molecules and significantly enhanced sensitivity due to the strong absorption cross sections. The sensors are rugged enough to be used under harsh conditions (e.g., supersonic combustion rigs), and they can be operated remotely via a computer interface.

Concentrations of NO and OH were measured in the vitiated airflow of a model scramjet combustor at Wright-Patterson Air Force Base in Dayton, Ohio. No absorption by OH was evident in the vitiated airflow, quantifying for the first time that the OH mole fraction is less than 0.2 ppm in the vitiated air used to simulate flight conditions in the scramjet facility. The results from these experiments validate previous studies in the scramjet facility, which have all assumed that OH is negligible in the vitiated airflow. For NO, diode-laser-based sensor measurements indicated that NO mole fractions of 180-1100 ppm were present in the vitiated airflow for vitiator stagnation temperatures of 1000-1389 K, respectively. NO absorption spectra were broader than predicted by 20% at all conditions, and a systematic shift of the line-center frequency to higher frequencies was observed with increasing vitiator stagnation temperature. No explanation has been identified for these two phenomena. Excellent signal-to-noise ratios were achieved with the sensor during the experiments, with a detection noise of 0.8% for a 2.5-second averaging time. In the vitiator exhaust conditions, this corresponds to a detection limit of approximately 2 ppm-m (at 500 K, 60 kPa).

Both sets of experiments represent the first application of diode-laser-based sensors for measurements of NO or OH in a model scramjet combustor. With knowledge of the concentrations of these two species in the vitiated airflow, researchers can examine the impact of vitiator contamination on the results of ground tests using the scramjet facility.

## Acknowledgments

The authors acknowledge the support of the Air Force Office of Scientific Research (AFOSR), Julian Tishkoff (Program Manager).

## References

- <sup>1</sup>R. B. Edelman and L. J. Spadaccini. Theoretical effects of vitiated air contamination on ground testing hypersonic airbreathing engines. *Journal of Spacecraft and Rockets*, 6:1442-1447, 1969.
- <sup>2</sup>B. Han, C. J. Sung, and M. Nishioka. Effects of vitiated air on hydrogen ignition in a high-speed laminar mixing layer. *Combustion Science and Technology*, 176:305-330, 2004.
- <sup>3</sup>C. J. Sung, J. G. Li, G. Yu, and C. K. Law. Chemical kinetics and self-ignition in a model supersonic hydrogen-air combustor. *AIAA Journal*, 37:208-214, 1999.
- <sup>4</sup>Y. Tan, C. G. Fotache, and C. K. Law. Effects of NO on the ignition of hydrogen and hydrocarbons by heated counterflowing air. *Combustion and Flame*, 119:346-355, 1999.
- <sup>5</sup>W. R. Laster and P. E. Sojka. Autoignition of H<sub>2</sub>-air: the effect of NO<sub>x</sub> addition. *Journal of Propulsion and Power*, 5:385-390, 1989.
- <sup>6</sup>T. Mitani. Ignition problems in scramjet testing. *Combustion and Flame*, 101:347-359, 1995.
- <sup>7</sup>T. Mitani, T. Hiraiwa, S. Sato, S. Tomioka, T. Kanda, and K. Tani. Comparison of scramjet engine performance in Mach 6 vitiated and storage-heated air. *Journal of Propulsion and Power*, 13:635-642, 1997.
- <sup>8</sup>T. Sander, A. Lyubar, T. Sattelmayer, and E. A. Shafranovsky. Influence of the burnout in vitiators on ignition limits in scramjet combustors. *AIAA Journal*, 42:319-325, 2004.
- <sup>9</sup>J. T. C. Liu, G. B. Rieker, J. B. Jeffries, M. R. Gruber, C. D. Carter, T. Mathur, and R. K. Hanson, "Near-infrared diode laser absorption diagnostic for temperature and water vapor in a scramjet combustor," *Applied Optics*, Vol. 44, No. 31, 6701-6711 (2005).

- <sup>10</sup>B. L. Upschulte, M. F. Miller, and M. G. Allen. Diode laser sensor for gasdynamic measurements in a model scramjet combustor. *AIAA Journal*, 38:1246-1252, 2000.
- <sup>11</sup>A. D. Griffiths and A. F. P. Houwing. Diode laser absorption spectroscopy of water vapor in a scramjet combustor. *Applied Optics*, 44:6653-6659, 2005.241
- <sup>12</sup>A. Mohamed, B. Rosier, D. Henry, Y. Louvet, and P. L. Varghese. Tunable diode laser measurements on nitric oxide in a hypersonic wind tunnel. *AIAA Journal*, 34:494-499, 1996.
- <sup>13</sup>S. F. Hanna, R. Barron-Jimenez, T. N. Anderson, R. P. Lucht, J. A. Caton, T. Walther, "Diode-laser-based ultraviolet absorption sensor for nitric oxide," *Applied Physics B*, Vol. 75, 113-117 (2002).
- <sup>14</sup>T. N. Anderson, R. P. Lucht, R. Barron-Jimenez, S. F. Hanna, J. A. Caton, T. Walther, S. Roy, M. S. Brown, J. R. Gord, I. Critchley, and L. Flamand. Combustion exhaust measurements of nitric oxide with an ultraviolet diode-laser-based absorption sensor. *Applied Optics*, 44:1491-1502, 2005.
- <sup>15</sup>T. N. Anderson, R. P. Lucht, T. R. Meyer, S. Roy, and J. R. Gord, "Diode-laser-based ultraviolet-absorption sensor for high-speed detection of the hydroxyl radical," *Optics Letters*, Vol. 30, 1321-1323 (2005).
- <sup>16</sup>T. R. Meyer, S. Roy, T. N. Anderson, J. D. Miller, V. R. Katta, R. P. Lucht, and J. R. Gord, "Measurements of OH mole fraction and temperature up to 20 kHz by using a diode-laser-based UV absorption sensor," *Applied Optics*, Vol. 44, No. 31, 6729-6740 (2005).
- <sup>17</sup>M. Gruber, J. Donbar, K. Jackson, T. Mathur, R. Baurle, D. Eklund, and C. Smith. Newly developed direct-connect high-enthalpy supersonic combustion research facility. *Journal of Propulsion and Power*, 17:1296-1304, 2001.
- <sup>18</sup>T. Mathur, M. Gruber, K. Jackson, J. Donbar, W. Donaldson, T. Jackson, and F. Billig. Supersonic combustion experiments with a cavity-based fuel injector. *Journal of Propulsion and Power*, 17:1305-1312, 2001.
- <sup>19</sup>T. N. Anderson, R. P. Lucht, S. Priyadarsan, K. Annamalai, and J. A. Caton, "In situ measurements of nitric oxide in coal-combustion exhaust using a sensor based on a widely-tunable external-cavity GaN diode laser," *Applied Optics* (in press).
- <sup>20</sup>T. N. Anderson, "Diode-Laser-Based Sensors for Flame Diagnostics and Combustion-Emissions Monitoring," PhD Dissertation, School of Mechanical Engineering, Purdue University, West Lafayette, IN, 2006.
- <sup>21</sup>Robert W. Fox and Alan T. McDonald. *Introduction to Fluid Mechanics*. 4<sup>th</sup> ed., John Wiley & Sons, Inc., New York, New York, 1992.
- <sup>22</sup>A. Y. Chang, M. D. DiRosa, and R. K. Hanson. Temperature dependence of collision broadening and shift in the NO A←X (0,0) band in the presence of argon and nitrogen. *Journal of Quantitative Spectroscopy and Radiative Transfer*, 47:375-390, 1992.
- <sup>23</sup>M. D. DiRosa and R. K. Hanson. Collision-broadening and -shift of NO  $\gamma(0,0)$  absorption lines by H<sub>2</sub>O, O<sub>2</sub>, and NO at 295 K. *Journal of Molecular Spectroscopy*, 164:97-117, 1994.